

An Open Database of Lunar Regolith and Simulants Properties

Léonie Gasteiner¹ | Naomi Murdoch¹ | Olfa D'Angelo^{1,2}

¹Institut Supérieur de l'Aéronautique et de l'Espace (ISAE-SUPAERO), Université de Toulouse, 10 Avenue Marc Pélegrin, 31055 Toulouse, France

²Van der Waals-Zeeman Institute, Institute of Physics, University of Amsterdam, Science Park 904, Amsterdam 1098XH, The Netherlands

Correspondence

Corresponding author: Olfa D'Angelo.
Email: olfa.d.angelo@isae-supaero.fr

Abstract

Lunar regolith, the layer of unconsolidated material covering the Moon's surface, is central to the science and technology developed for the Moon, notably related to *in-situ* science investigations, resource utilization, surface infrastructure, and mobility systems. However, data on lunar soil properties remain fragmented across decades of mission reports, often in formats that are difficult to access or interpret. We present a newly compiled database of lunar regolith physical and geotechnical properties, including data collected by direct *in-situ* measurements from crewed missions, estimates inferred from surface interactions on the Moon and using remote sensing, as well as laboratory analyses of samples returned to Earth. The data collected include, among others, the angle of internal friction and cohesion (both Mohr-Coulomb model parameters), bulk density, and static bearing capacity, extracted from Luna and Apollo-era historical mission documentation all the way to contemporary Lunar programs. The dataset specifies the type and location of the tests from which each value was obtained. Our database also includes parameters for lunar regolith simulants, providing a direct link between mission data and laboratory studies. In addition to centralizing this information, we developed a user interface that facilitates data retrieval, filtering, and visualization. This interface enables users to generate customized plots for comparative analysis. Developed in an open-science perspective, it is designed to evolve in response to the community's needs. The database and its associated tools significantly enhance the accessibility and usability of lunar regolith and simulants data for scientific and engineering research.

KEY WORDS

Moon, Lunar Regolith, Lunar Regolith Simulant, Database, Soil Mechanics, Open Science

1 | INTRODUCTION

The physical and geotechnical properties of lunar regolith govern a wide range of processes, from rover mobility to landing site selection, excavation strategies, instrument design and construction methods on the Moon [1]. With the renewed interest in lunar exploration, driven by NASA's Artemis program [2], the emergence of commercial actors [3], and the growing number of nations pursuing independent lunar missions [4–8], a new generation of scientists and engineers is turning to existing data on the lunar surface.

For these users, there is a growing need for data that are accessible, comparable, and interpretable. Because of the high ecological and economic costs of space missions, all available data are highly valuable. Much of our current understanding stems from the Apollo-era missions, notably compiled in the Lunar Sourcebook [9]. More recent missions [5–8] but also re-interpretation of existing data [9–11] are now expanding

this foundation. Yet, many critical parameters remain difficult to retrieve. This is largely due to the decentralized and heterogeneous nature of historical lunar mission data. Typically, reports from the Apollo, Luna, and Surveyor programs are often embedded in incompatible formats, dispersed across archives, or accessible only through scanned documents in their original language, which complicates their integration, comparison, and analysis. This fragmentation hinders both the advancement of lunar science and the reinterpretation of existing results using modern analytical tools.

In line with recent efforts to revisit Apollo-era datasets and reconstruct a consistent picture of lunar soil mechanics [12, 13], our work integrates data ranging from 1966 with the Luna 9 mission report [14], to 2025 with a paper on the Chandrayaan-3 mission [5]. The database includes results from direct *in-situ* testing during crewed missions [15–20]; estimations derived from surface interactions such as rover tracks [17, 18, 20–22], astronaut footprints [19], lander padprints [15, 16, 23–26]; and remote sensing data [27, 28].

Data on lunar regolith simulants are also included [29–47]. Such materials are essential for testing technologies and experimental methods intended for lunar applications. However, their mechanical and rheological properties often differ significantly from those of true lunar regolith, especially from true lunar regolith as found *on the Moon*. The development of improved simulants requires a robust ground-truth reference – or rather, a *Moon-truth*.

In addition to the geotechnical results themselves, our database specifies the type of test used to measure each parameter (e.g. penetrometer, rover tracks analysis, direct shear test, etc.). In an effort towards greater reproducibility, when available, complementary details, such as the unconsolidated bulk density or the range of normal stresses applied in the Mohr-Coulomb analysis, are included. When relevant and available, it also includes contextual information, such as the geographical coordinates of *in-situ* tests, local gravitational acceleration, and environmental conditions during experiments. This information is particularly relevant given the increasing recognition that reduced gravity, among other aspects of the lunar environment, significantly influence granular behavior [48–55].

This article is organized as follows: Section 2 proposes a guide to quickly start using the database. Section 3 describes the structure and methodology underlying it, including data selection and formatting choices. Section 4 presents three example use-cases that illustrate how the database can support current and future research. Finally, in Section 5, we discuss the limitations of the current version and outline directions for future development, emphasizing the importance of community engagement in fostering an open-science framework for lunar geotechnical research.

2 | QUICK START

The Lunar Regolith Database is openly accessible via a web application hosted on the Streamlit platform at <https://lunar-regolith-database.streamlit.app/>. Access requires only an internet connection and a web browser.

For users who wish to run the database locally, the full repository containing both the source code and the dataset can be downloaded from <https://github.com/leoniegasteiner/Lunar-Regolith-Database>. Detailed installation and usage instructions are provided in the accompanying `README.md` file. A concise overview is given below.

2.1 | Requirements

To run locally, the database requires Python (version 3.9–3.12) and the following packages: `streamlit`, `pandas`, `numpy`, `plotly`, `re`, `base64`, `importlib`, and `os`. The application

runs in any modern browser (Chrome, Firefox, Safari, or Edge) and does not require an internet connection once installed locally.

2.2 | Execution

To launch the application, navigate to the project directory in a terminal and execute the following command:

```
streamlit run Lunar_Database.py
```

The application will automatically open in the default browser. Alternatively, it can be accessed manually through the local URL provided in the terminal output.

3 | METHODOLOGY

3.1 | Data sources and extraction

We systematically reviewed technical documents from multiple lunar missions, prioritizing those that reported *in-situ* measurements and laboratory analyses of returned samples. Key sources included:

- NASA Surveyor (1966 - 1968) preliminary science reports [23–26, 56];
- NASA Apollo mission (1969 - 1972) technical reports [15–20];
- Soviet Luna mission (1966 - 1976) summaries [11, 14, 21, 57];
- Recent mission publications, including data from the Chang'E and Chandrayaan programs [5, 6, 8, 58].
- Later interpretations of lunar data [9–11]

Data extraction was performed manually to ensure accuracy, given the often qualitative and sometimes unstructured nature of original sources. For *in-situ* lunar data, each entry in the database includes metadata specifying the mission, testing method, geographic location (latitude and longitude on the Moon), and the corresponding reference source. The “location” field provides the lunar coordinates of the mission landing. For data obtained on Earth from returned lunar samples, the database records the mission responsible for sample return, and the location of the landing on the moon. A clear distinction between *in-situ* surface measurements and post-mission, ground-based analyses is maintained through the “test location” field, distinct from “location”: the test location is either “*in-situ*”, “on Earth”, or “remote” for remote sensing missions data.

For regolith simulants, the database includes the developer, year of creation, simulant type (mare or highland), and the corresponding mechanical parameters derived from the lunar regolith when available. A dedicated page within the database, accessible via a button in the main filter panel, provides access to simulants data through a searchable table and several visualization options. To facilitate direct comparison between simulants and actual lunar regolith, both datasets report the same main physical parameters.

A comprehensive table combining lunar regolith and simulant data is also available for download from the main interface. Users can apply filters to tailor the displayed data to their specific research needs.

A page displaying details about each specific missions context and data can also be accessed through the main filter panel. It elaborates on the context of each mission's test and sample analysis. All the data collected during that specific mission is displayed in a table.

General interpretations of lunar regolith are often included in the different mission reports and reinterpretation papers, these values corresponding to general parameters for bulk lunar regolith are included in a different page in the database.

The physical parameters included in the database were extracted from multiple sources, beginning with the earliest available reports and incorporating subsequent interpretations when possible. When several values were reported for the same parameter, mission, and testing method, all were retained to provide a comprehensive overview of the data. The year of publication was also recorded to help users assess the evolution of interpretations over time.

3.2 | Parameters

The current version of the database includes (but is not limited to):

1. Angle of internal friction (in degrees); first parameter in the Mohr-Coulomb model, corresponding to the slope of the Coulomb failure line [59];
2. Cohesion (Pa); second parameter in the Mohr-Coulomb model, corresponding to the intercept of the Coulomb failure line with the shear strength axis [59];
3. Bulk density (g cm^{-3}); defined as the mass of unconsolidated regolith per unit volume;
4. Bearing capacity (kPa); defined as the maximum load per unit area that the regolith can support without failure;
5. Normal stress range (kPa); range of normal stresses applied during shear testing of returned samples on earth from which the Mohr-Coulomb parameters were derived;
6. Test; the measurement method used, currently among the ones described in Sec. 3.3;

7. Measurement location; for *in-situ* data, documented location on the Moon where the measurement was conducted;
8. Test location; indicates whether the measurement was performed *in-situ* on the lunar surface, on Earth using returned samples, or remote for remote sensing data;
9. Reference; bibliographic citation of the source from which the data were extracted;
10. Depth; depth below the lunar surface at which the measurement was taken, when available;
11. Force applied; for penetrometer tests, the force applied during the test, when available;
12. Porosity (%), void ratio, density of grains (g cm^{-3}), and compressibility coefficient; additional parameters reported when available.

The database will continue to be updated over time, reflecting new findings and contributions. In line with our commitment to open science, we actively invite researchers to contribute their own data, particularly on existing or novel lunar regolith simulants. To ensure the scientific integrity and reproducibility of the database, all submitted data must meet the following criteria: The data must be published in a peer-reviewed, non-predatory journal. The testing methodology must be clearly described. If no detailed protocol is available in the publication or online, contributors are required to provide a comprehensive description of the procedure. For all datasets currently included in the database, the associated testing methods are described in detail in the sections below.

3.3 | Testing methods classification

The database categorizes the data obtained on the Moon according to the testing methodology used. Due to the limited number of experiments that could be performed *in-situ*, no two investigation methods were identical. The data were therefore divided according to the general procedure used to obtain them. The paragraphs below describe the terminology used for the classification of these testing methods, the general procedure they represent, and the missions in which they were applied. The different testing methods are classified depending on the testing location; *in-situ*, on earth, or remote sensing.

3.3.1 | In-Situ testing methods

Spacecraft Touchdown Analysis & Vernier Thrusters:

Spacecraft touchdown analysis was the first method used to retrieve data on the mechanical properties of the lunar regolith. It was applied during most lunar missions; however, numerical values were only determined for the Surveyor missions I, III, V, and VI, as well as the Apollo

11 and 12 missions [15, 16, 23–26]. The method consists of analysing the appearance of the lunar surface near the lander footpads through photographs taken after disturbance, together with the histories of axial loads recorded in the shock absorbers of each leg during landing. Similarly, the Vernier thrusters analysis was performed during the Surveyor VII mission [56], where the lander was equipped with vernier thrusters used for fine control during descent and landing. The analysis of the interaction between the thruster plumes and the lunar surface provided additional information on the regolith's mechanical properties.

Trench Experiment: Trench tests were performed using the lunar sampler of the Surveyor VII mission and by the astronauts of the Apollo 14 and 15 missions [17, 18, 56]. The test consisted of scooping portions of lunar regolith and observing the angle of repose and the general behavior of the material when digging into it.

Optical Assessment: The optical assessment method was primarily used during the Luna 9 mission [14], which involved taking photographs of the lunar surface. No numerical data on the mechanical properties of the regolith were retrieved using this method.

Penetrometer: Penetrometer experiments were first performed during the Luna 13 mission [21], whose lander was equipped with a mechanical punch penetrometer that provided numerical data on the top layer of the lunar surface. Subsequent penetrometer experiments were conducted by the Soviet rover Lunokhod I, deployed by the Luna 17 mission [11], allowing data collection in regions with undisturbed surface soil. Similar experiments were also performed by the astronauts of the Apollo 14, 15, and 16 missions [17–19]. These experiments consisted of recording the force required to insert a device into the regolith to a given depth.

Rover Tracks & Footprint Analysis The observation of rover tracks provides valuable insight into the behavior of lunar regolith. Such observations began with the Lunokhod I and II rovers from the Luna 17 and 21 missions [11, 21] and continued with the Apollo 14, 15, and 17 missions [17, 18, 20], as well as more recent missions such as Chang'e 5 [6]. Although the Apollo 14 mission did not include a rover, similar observations were made using the tracks of the Modular Equipment Transporter (MET). This technique involves focusing cameras on the rover wheels to observe the interaction between the wheels and the lunar surface. It allows estimation of regolith density and internal friction angle, although cohesion values are often assumed from prior experiments.

Footprint analysis was performed during the Apollo 11, 12, 14, and 15 missions [15–18]. This method involves analyzing the depth and shape of astronaut footprints on the lunar surface to infer mechanical properties of the regolith.

Core Tube, Drive Tube, Drill Core, & Drill Stem: Core tube, drive tube, drill core, and drill stem methods were employed during the Luna 16, 20, and 24 missions [11, 21, 60], as well as the Apollo 15 and 16 missions [18, 19]. These methods involve extracting cylindrical samples of lunar regolith using various drilling techniques. The samples are then analysed to determine properties such as bulk density and cohesion. Although these methods were primarily used for sample collection, they also provided indirect information on the mechanical properties of the regolith through the behavior of the regolith during and after sampling.

Other Testing Methods: With more recent lunar missions, new technologies have enabled the design of dedicated experiments. For the sake of simplicity and due to the limited availability of recent data, these methods are not detailed in this paper. Notable examples include the Lunar Penetration Radar of the Chang'e 3 mission [58] and the Surface Thermophysical Experiment of the Chandrayaan-3 mission [5], which are documented in the references cited in the database.

3.3.2 | On-Earth testing methods

Core Tube & Drill Core: Core tube and drill cores brought back to Earth by the Apollo and Luna missions were tested using various techniques, mainly analysing the chemistry and grain size distribution. One important value taken directly from these samples is the bulk density of the regolith.

Direct Shear, Triaxial Shear, & Rotational Shear: These testing methods are standard geotechnical laboratory tests used to determine the shear strength parameters of soils. The direct shear test involves applying a horizontal force to a soil sample until failure occurs, allowing for the determination of cohesion and internal friction angle. The triaxial shear test subjects a cylindrical soil sample to axial and confining pressures, providing a more comprehensive understanding of soil behavior under different stress conditions. The rotational shear test involves applying a torque to a soil sample to measure its shear strength.

Rotating Drum: Rotating drum tests were conducted on samples brought back by the Luna 16 and 20 missions [21]. They consist of observing the behavior of regolith when placed in a rotating cylinder, allowing for the determination of the material's dynamic angle of repose.

3.3.3 | Remote Sensing testing methods

Boulder Tracks: Boulder track analysis was performed using images captured by lunar orbiters, such as the Lunar Reconnaissance Orbiter (LRO) [27, 28]. This method involves studying the tracks left by boulders rolling down slopes to infer the mechanical properties of the regolith, such as the internal friction angle. They often require assumptions based on prior *in-situ* measurements to estimate numerical values of cohesion or bulk density.

3.4 | Database Architecture

The global architecture of the database is represented in Figure 1. It runs through a main python script that integrates all functionalities, including data filtering, visualization, and export options. The data is stored in .csv format in `Dataset_Regolith` for true lunar regolith data, `Dataset_Simulants` for simulants data, `Dataset_All` for data of lunar missions and simulants combined, and `Dataset_General` for averaged values of the bulk behavior of lunar regolith. In the same folder, a `requirements.txt` file lists all necessary Python packages to run the database locally, a `README.md` file with installation and usage instructions, and a image `moon_map.jpg` [61] allowing for the lunar map visualization. Finally, a folder titled `Pages` contains the individual scripts for each mission reported in the database, providing more in-depth information on the context of data collection.

The database is accessible as a web application via a direct link (<https://lunar-regolith-database.streamlit.app/>) or by running a Python script developed with the `streamlit` package, which enables interactive data visualization through a web browser. The main script is located in a dedicated folder alongside supporting documents containing the raw datasets.

The database is organized into five main pages:

1. **Lunar regolith data:** This first page compiles all data collected from the various lunar missions. It includes:

- A searchable and sortable table containing metadata such as mission name, testing method, location, physical parameters, and reference source.
- An interactive plotting section with drop-down menus for selecting parameters and defining visualization

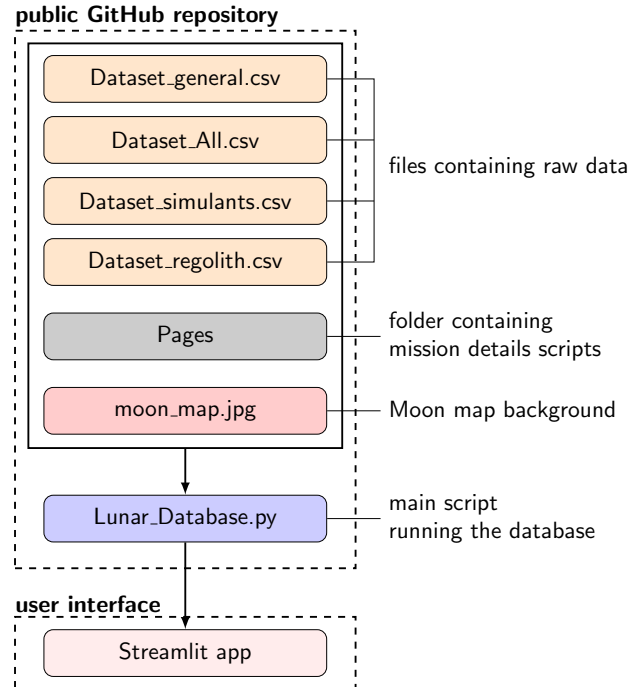


FIGURE 1 Schematic of the database architecture. Overview of the data files, processing scripts, and user interface forming the lunar regolith database.

modes (e.g., data ranges, minimum values, maximum values, or averages) with customizable legends.

- A filter panel (on the left side of the interface) that allows users to refine the displayed data according to specific criteria (e.g., mission, testing method, location, or parameter range).
- A lunar map displaying the geographic location on the Moon of each mission.

2. **Lunar regolith simulants data:** Accessible via a button at the top of the filter panel, this page provides data on lunar regolith simulants and includes:

- A table compiling metadata for each simulant, such as developer, year of creation, simulant type (mare or highland), physical parameters, and reference source.
- An interactive plotting section and filter panel identical in functionality to those of the regolith data page, enabling comparative visualization.

3. **Combined dataset:** This page, also accessible via the top navigation button, presents a unified table merging lunar regolith and simulant data. It allows:

- Direct comparison of both datasets through a single table containing mission, testing method, location, physical parameters, and reference information.
- Filtering capabilities to refine the dataset according to user-defined criteria.

4. General interpretations of bulk lunar regolith: Accessible via a button at the top of the filter panel, this page provides data on average bulk behavior of lunar regolith. It contains:

- A table compiling metadata for reported general values of parameters such as cohesion, bulk density, and angle of internal friction. The corresponding source for each set of parameters is specified.
- An interactive plotting section and filter panel identical in functionality to those of the regolith data page, enabling comparative visualization.

5. Mission details: The final page provides descriptive information on each mission included in the database. It features:

- A filter panel for selecting a specific mission.
- A section displaying general mission information, such as landing date, location, and primary scientific objectives.

All tables, filtered or not, can be exported directly from the interface in .csv format.

4 | USE-CASES

We illustrate typical applications of the database through three representative use-cases. The tools implemented for filtering and visualization enables real-time updates of plots based on user-defined constraints, facilitating data exploration. It also allows for rapid visual comparisons that can support model calibration or guide the interpretation of experimental results. Here, data are filtered, then extracted directly from the database in .csv format and replotted, as can be done by any ordinary user.

In the following, we always use the term “cohesion” as the intercept in Mohr-Coulomb, not as a direct measurement of interparticle cohesive forces.

4.1 | Use-case 1: Comparing soil mechanics measured *in-situ* across lunar terrains

The lunar surface is broadly divided into two main terrain types: highlands and maria. The maria are relatively flat with low albedo, while the highlands are heavily cratered and mountainous with significantly higher albedo. Their formation processes explain their different topography, but also different chemical compositions: the highlands are dominated by feldspathic rocks, whereas the maria consist mainly of basaltic lavas rich in pyroxene [62]. Besides, localized lunar pyroclastic deposits, produced by explosive volcanic eruptions, are widespread across the Moon, occurring in both mare and highland regions [63]. Figure 2 presents a global Moon map, illustrating the contrast between the dark maria and the lighter highland regions, including mission landing sites. This map is extracted directly from the database.

This distinction in geological evolution is also reflected in different regolith physical properties. Using the database, we investigate whether these different physical properties result in distinct mechanical responses. We generate two datasets, based only on *in-situ* measurements, but collected by any testing method: one with only measurements from mare sites and another from only highland sites. In Figure 3, we generate side-by-side visualizations of internal friction angle and cohesion (both Mohr-Coulomb model parameters), both plotted as a function of bulk density, for the two terrain types.

The Apollo missions program provided the first opportunity to systematically investigate these terrain types through sampling and *in-situ* experiments. The Apollo 11, 12, 15, and 17 missions landed in mare regions, while the Apollo 14 and 16 missions targeted highland terrains. Figure 4 shows spatial spread of the location of data collection (note that it includes non-Apollo missions).

The Apollo 14 mission was the first of the program to explore lunar highland terrains, landing in the Fra Mauro formation. The properties of the soil during this mission were directly compared to those of the Apollo 11 and 12 missions, which had landed in mare regions. The results of the trench experiment [64] indicated that the highland regolith exhibited a much lower cohesion than that of the mare sites. The bulk density of the highland soil was also found to be lower than that of the mare sites, with a value of approximately 1.5 g cm^{-3} for the highlands, compared to 1.75 g cm^{-3} for the mare sites.

The Apollo 15 mission landed in a mare region and reported a bulk density of approximately 2.0 g cm^{-3} , higher than that of the Apollo 14 highland site [65]. The values of the angle of internal friction for the Apollo 15 mare regolith ranged from 41 to 52 degrees, compared to approximately 35 degrees for the Apollo 14 highland site [65]. The Apollo 16 mission, which landed in the Descartes highlands, provided further data on

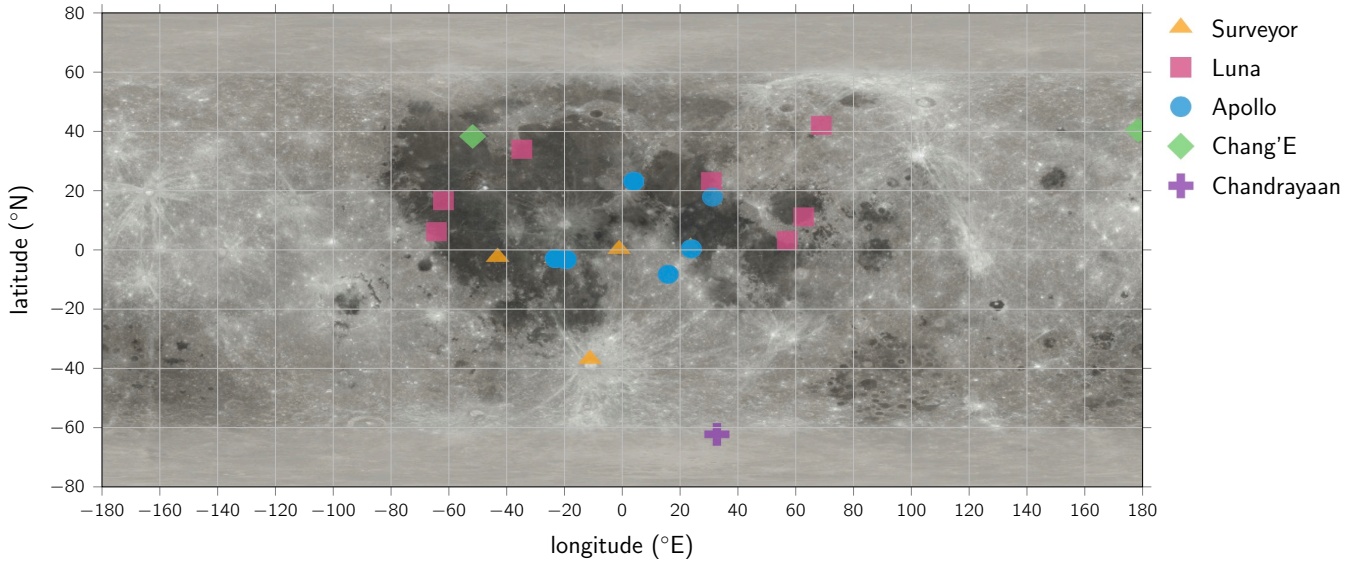


FIGURE 2 **Moon map with missions landing sites.** The global lunar albedo map shows the contrast between the dark lunar maria and the lighter highland regions. The cylindrical projection uses the selenographic coordinate system, spanning from -180°E to 180°E (left to right) and 90°N (North pole, top) to 90°S (South pole, bottom), centered on the mean sub-Earth point (0°N , 0°E). The map is reproduced with permission from NASA's Scientific Visualization Studio CGI Moon kit [61]. Each mission landing site is placed on the map (see legend for specific mission identification). This map, including the mission landing sites, is directly extracted from the database website.

highland regolith properties. The bulk density measured at this site was approximately 1.7 g/cm^3 , displaying no significant difference with mare values. The angle of internal friction for the Apollo 16 highland regolith was around 46 degrees, again more similar to mare measurements than to highland regolith properties [66]. The last mission of the program, Apollo 17, landed in the Taurus-Littrow valley, a region characterized by both mare and highland features. The bulk density measured at this site was approximately 1.6 g cm^{-3} , while the angle of internal friction was found to be around 35 degrees [67]. These values were more consistent with mare regolith properties than with those of highland terrains.

Overall, the data from the Apollo missions reveal a large diversity among different results and locations on the Moon, even within each terrain type. It suggests that while some differences in regolith properties exist between mare and highland terrains, these differences may not be as pronounced as initially thought. The angle of internal friction, cohesion and bulk density values for highland sites (Apollo 14 and 16) were found to be closer to those of mare sites (Apollo 11, 12, 15, and 17) than previously reported in earlier missions such as Surveyor VII. This finding indicates that local geological processes and impact history may play a more significant role in determining regolith properties than the broad classification of terrain type alone. Based on the accessible *in-situ* measurements, the type of lunar terrain does not appear to induce strong differences

in geomechanical soil properties, at least with respect to the parameters commonly used to characterize lunar soil.

A similar conclusion was drawn from observations of boulder tracks on the lunar surface: a qualitative comparison of track morphology across mare, highland, and pyroclastic deposits revealed no significant differences in their appearance, suggesting comparable geomechanical properties of the underlying materials [68].

In conclusion, we do not observe a clear distinction – either because the intrinsic variability of lunar soil is larger than the differences between specific terrain types, or because the testing conditions and environments differ so much that these variations overshadow any real geological distinctions. The lack of repeated measurements on the same location and with the same methods ultimately prevents us from identifying the true origin of the discrepancies.

In contrast, we see that soil bulk density emerges as a more characteristic parameter influencing geomechanical lunar soil properties. The density and mechanical strength of lunar regolith are known to vary with depth; understanding this variation based on existing *in-situ* data is essential for predicting load-bearing capacity, excavation resistance, and stability during surface operations.

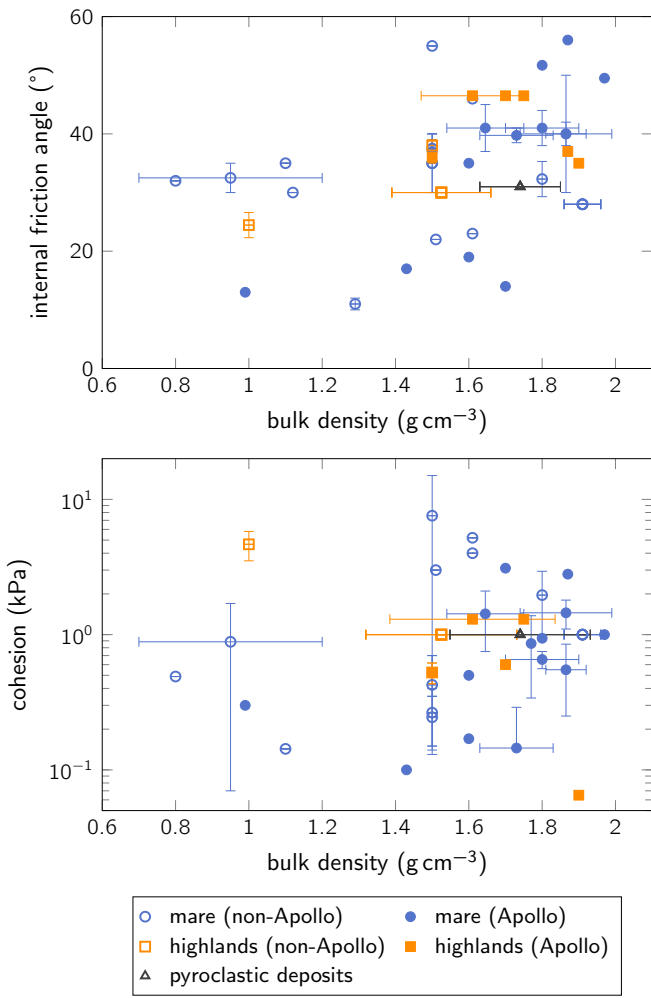


FIGURE 3 Geomechanical properties of lunar regolith depending on type of lunar terrain. Internal friction angle (top) and cohesion (bottom), both parameters of the Mohr-Coulomb failure model, are shown as functions of bulk density. Cohesion values are plotted on a logarithmic scale (y-axis) to capture their wide range, spanning two orders of magnitude, from 100 Pa to 10 kPa. Filled symbols indicate data obtained during the Apollo missions, while open symbols represent data from all other missions.

4.2 | Use-case 2: Comparing *in-situ* data to returned samples measured on-ground

The lunar environment differs profoundly from that we know on Earth: its surface gravity is only one-sixth of Earth's, it is surrounded by a thin surface-bound exosphere close to vacuum, and it undergoes regular micrometeoroid impacts in the absence of an atmosphere; it also lacks active weathering processes. These factors shape the physical and mechanical behavior of lunar regolith in ways that have no terrestrial analogue. But beyond how these conditions modify the material

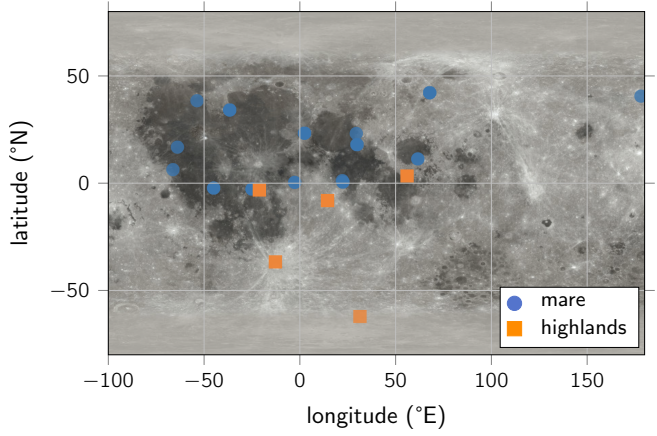


FIGURE 4 Moon map showing the geographic locations of missions as a function of lunar terrain. Locations are classified as mare (blue disks) and highland (orange squares); the points highlight the spatial spread of the location of data collection.

itself, the testing environment may also affect measurement results.

The influence of gravity on granular behavior is now well established [49, 51, 55]. Here, we adopt a broader perspective: using data from previous missions, we assess whether geomechanical tests conducted *in-situ* on the lunar surface yield systematically different results from tests performed on returned samples.

In Figure 5, we pool results from all missions, ignoring differences in test type and sampling location on the Moon. Although the database makes these finer-grained analyses readily accessible, our goal here is more global: to evaluate whether lunar measurements diverge systematically from Earth-based geomechanical properties measurements. We also include the dataset based on remote observations of boulder tracks [68], which estimates cohesion at a fixed 1 kPa.

We see a clear pattern emerge: *in-situ* lunar data exhibits higher internal friction angles and often lower cohesion compared to measurements performed on returned samples. While the internal friction angle generally increases with bulk density, the relationship between cohesion and bulk density appears far less systematic.

Regarding bearing capacity, values estimated from boulder-track observations are up to one order of magnitude larger than those from experiments conducted directly on the lunar surface. This discrepancy must be attributed to differences in the tested material properties or the distinct measurement methods employed.

Finally, across all parameters considered, on-Earth measurements display substantially broader variability, underlining the

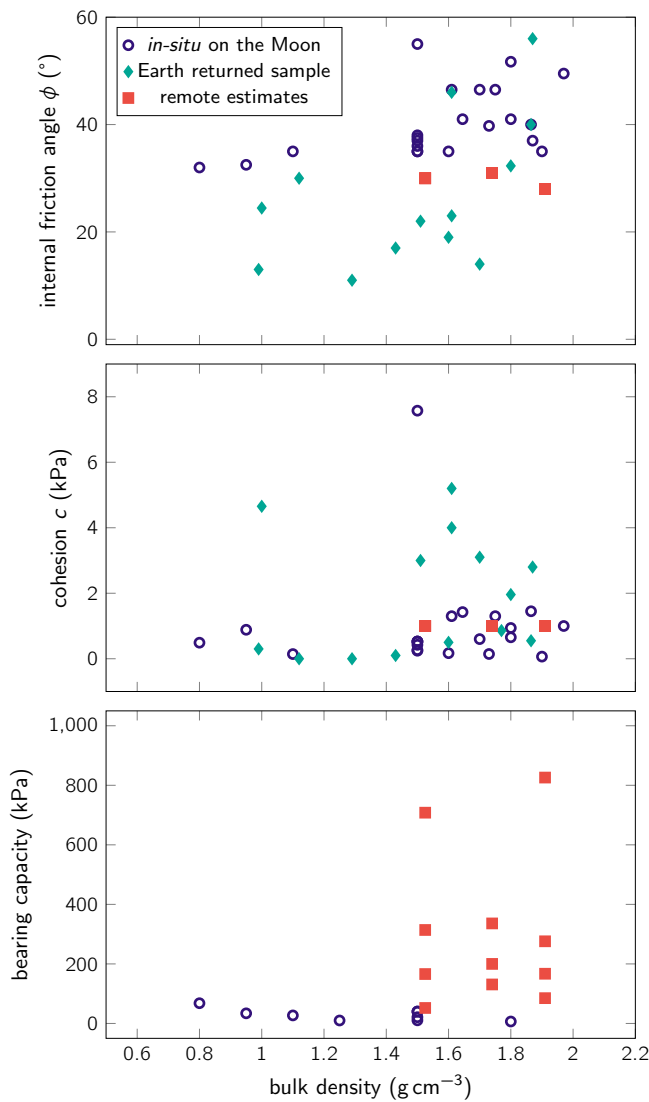


FIGURE 5 Comparison of geomechanical properties measured on Earth versus the Moon. We compare three typical geomechanical properties (internal friction angle, cohesion, bearing capacity), as a function of bulk density, for true regolith tested *in-situ*, returned samples tested on ground, and properties estimated remotely.

strong influence of environmental conditions. This is a key issue in granular physics (and soft matter more broadly): because such materials are highly sensitive to gravity, what we often regard as an intrinsic property of the material can be, in practice, a characterization of the material *within its environment*. While this might not be inherently problematic, it becomes crucial to keep in mind when planning missions to markedly different environments, as material properties may scale in fundamentally different ways from one environment to another.

4.3 | Use Case 3: Selecting an appropriate lunar simulant

Lunar regolith simulants have been developed for decades to reproduce the behavior of lunar soil for laboratory and engineering studies. Many lunar regolith simulants focus primarily on reproducing one or a few properties of true lunar regolith, for example its chemical composition, optical properties or particle size distribution. Depending on the specific process tested, it can be either perfectly sufficient or entirely inadequate.

For example, challenges during *in-situ* experiments might be traced back to using simulants with inappropriate mechanical properties. During Apollo 15, astronauts encountered unexpected struggles with drill penetration and deep core sample retrieval, due to “unexpectedly hard material approximately 1 m below the surface” [69]. The drill stems did not penetrate at expected rates, and underwent mechanical dysfunction due to torques that were much higher than expected following testing on-ground, in terrestrial soil. Concretely, extracting the deep core sample required both crewmen lifting on the drill handles, costing far more time and effort than planned, and ultimately limiting the crew’s ability to explore other Moon locations [69].

This example illustrates the importance of having knowledge about the mechanical properties and behavior of the lunar surface when designing a mission. To test tools or scientific instruments to be used on the Moon, it is often particularly useful to know which lunar simulant is most representative of a particular region of the Moon, in flow or mechanical properties. Appropriate lunar simulants can also help to improve the planning of operations and to interpret acquired data.

The database includes data for existing simulants, enabling direct comparisons with either lunar regolith or other available simulants. Due to the large number of existing simulants, as well as the rate at which new simulants are produced and (partially) characterized, it is challenging to maintain a comprehensive and up-to-date catalogue referencing all available simulants. We focus on widely-used simulants whose characterization has been published in peer-reviewed articles, and update the list based on individual requests, provided that the characterization data has been previously published in a peer-reviewed article.

In Figure 6, we see that the cloud of points corresponding to true lunar regolith tested on the Moon is clearly below that of regolith simulants, showing materials with lower cohesion, albeit relatively similar angle of internal friction. Focusing specifically on cohesion, we see that a lower cohesion in the Mohr-Coulomb sense does not seem to be directly correlated with a lower bulk density.

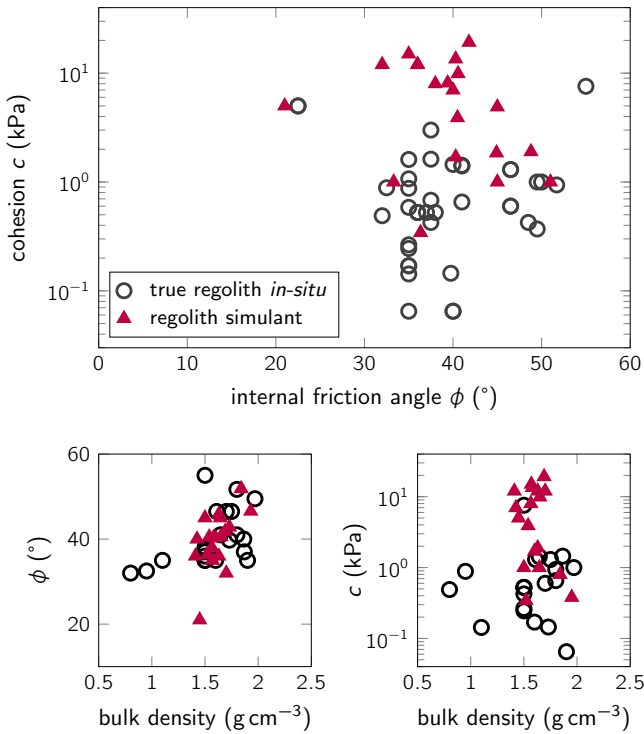


FIGURE 6 Comparison of true regolith *in-situ* to regolith simulants, tested on Earth. angle of internal friction angles of lunar regolith and lunar simulants.

A possible explanation lies in the particles' morphology: lunar regolith particles tend to be highly angular and geometrically complex, leaving more void space between particle surfaces. This reduces the number of true contact points, thereby weakening surface-dominated cohesive forces, even at equivalent bulk densities.

This comparison also highlights an important limitation of terrestrial regolith simulants. Because their formation processes differ fundamentally from those of lunar materials, simulants diverge in certain properties. It is therefore essential to identify and reproduce the *relevant* physical parameters as faithfully as possible; otherwise, mission preparation performed in an inappropriate simulant risks leading to unexpected failures on planetary surfaces.

5 | DISCUSSION

5.1 | Data Coverage and Tool Performance

The current version of the Lunar Regolith Database includes over 200 entries spanning all six Apollo landing sites, several Luna mission sites, and selected robotic mission data. The dataset covers bulk density values ranging from 0.7 g cm^{-3} to

2.3 g cm^{-3} , angles of internal friction from 20° to 55° , and cohesion from negligible up to approximately 5 kPa , depending on sampling depth and location. Coverage varies by parameter and mission: for example, most bulk density measurements come from Apollo core samples, while cohesion and internal friction are more frequently derived from penetrometer and trench experiments.

The interactive filtering and visualization tool allows users to explore this dataset efficiently, generating plots and maps in real time based on selected constraints. For instance, researchers can quickly compare regolith properties across Mare and Highland terrains, examine depth-dependent trends, or identify suitable simulants for laboratory experiments. The platform thus provides a critical bridge between historical mission data and contemporary analytical and engineering needs.

5.2 | Limitations and Uncertainties

While the database significantly improves accessibility and standardization of lunar regolith data, several limitations remain. The precision and accuracy of the original measurements vary widely due to differences in mission instrumentation, sampling methods, and experimental conditions. Some values, particularly those derived from touchdown analyses or optical observations, are indirect estimates rather than direct measurements. Future work will include uncertainty quantification and expansion to incorporate remote-sensing derived properties and analog simulant data for laboratory validation.

Additionally, the database currently focuses on mechanical properties measured *in-situ* or from returned samples. Expanding the database to include returned samples experiments and results, chemical composition and other properties would further enhance its utility for scientific and engineering applications.

5.3 | Future Work

The database is intended to evolve in time. Future updates will include data from upcoming missions such as Artemis and Chang'E 6–7, additional laboratory analyses of regolith simulants, and remote-sensing derived properties that can fill existing spatial gaps. We also envision integrating this tool with planetary GIS platforms and simulation environments for *in-situ* resource utilisation (ISRU) systems, lunar base planning, and regolith processing technologies.

Community contributions are actively encouraged, provided that submitted data meet established quality and documentation standards.

6 | CONCLUSION

We present a consolidated and accessible database of lunar regolith properties, paired with an interactive interface for data exploration and visualization. By centralizing decades of mission data and enabling rapid filtering, mapping, and comparison, the database supports both retrospective scientific analysis and forward-looking mission design.

The use-cases presented illustrate practical applications of the tool for research and engineering. Beyond facilitating fundamental studies in planetary science, this database has direct relevance for rover mobility analysis, lander design, ISRU system planning, and lunar construction activities.

As an open-access resource, the Lunar Regolith Database is designed to evolve with new mission data, laboratory studies, and community contributions, providing a growing foundation for safe and efficient exploration of the Moon.

ACKNOWLEDGMENTS

N. M. acknowledges funding from the European Research Council (ERC) GRAVITE project (Grant Agreement № 1087060).

O. D'A. acknowledges financial support from the French National Centre for Space Studies (CNES) under the CNES fellowship 24-357 and APR № 10678 (2025).

REFERENCES

- Yusuf Cengiz Toklu, Pinar Akpinar, *Advances in Space Research* **70**(3), 762 (2022).
- Sarah Noble, Brad Bailey, Jeff Grossman, Paul Hertz, Amanda Nahm, Debra Needham, Katharine Robinson, Kathleen Vander Kaaden, Ryan Watkins, Shoshana Weider, *Implementation Plan for a NASA Integrated Lunar Science Strategy in the Artemis Era* (2024), NTRS Author Affiliations: National Aeronautics and Space Administration, National Aeronautics and Space Administration (Retired), Arctic Slope Regional (United States), Arctic Slope Technical Services NTRS Document ID: 20240015059 NTRS Research Center: Headquarters (HQ). <https://ntrs.nasa.gov/citations/20240015059>.
- Yangting Lin, Wei Yang, Hui Zhang, Hejiu Hui, Sen Hu, Long Xiao, Jianzhong Liu, Zhiyong Xiao, Zongyu Yue, Jinhai Zhang, Yang Liu, Jing Yang, Honglei Lin, Aicheng Zhang, Dijun Guo, Sheng Gou, Lin Xu, Yuyang He, Xianguo Zhang, Liping Qin, Zongcheng Ling, Xiongyao Li, Aimin Du, Huaiyu He, Peng Zhang, Jinbin Cao, Xianhua Li, *Science Bulletin* **69**(13), 2136 (2024).
- Jessica Flahaut, Carolyn H. van der Bogert, Ian A. Crawford, Sébastien Vincent-Bonnieu, *npj Microgravity* **9**(1), 50 (2023).
- Nizy Mathew, K. Durga Prasad, Dinakar Prasad Vajja, V. Aasik, Fazil Mohammad, P.P. Pramod, M. Satheesh Chandran, Kiran John Antony, M. Ram Prabhu, M.B. Dhanya, Manu V. Unnithan, Shiju G. Thomas, Chandan Kumar, Dona Mathew, R. Suresh, K.P. Subhajayan, P.S. Ajeeshkumar, P. Kalyana Reddy, Samik Jash, K. Kannan, K. Sunitha, Sanjeev Mishra, Janmejay Kumar, V. Sathiyamoorthy, Anil Bhardwaj, *Advances in Space Research* **75**(7), 5936 (2025).
- Chunlai Li, Hao Hu, Meng-Fei Yang, Zhao-Yu Pei, Qin Zhou, Xin Ren, Bin Liu, Dawei Liu, Xingguo Zeng, Guangliang Zhang, Hongbo Zhang, Jianjun Liu, Qiong Wang, Xiangjin Deng, Caijin Xiao, Yong-gang Yao, Dingshuai Xue, Wei Zuo, Yan Su, Weibin Wen, Ziyuan Ouyang, *National Science Review* **9**(2), nwab188 (2022).
- Zehua Dong, Guangyou Fang, Yicai Ji, Yunze Gao, Chao Wu, Xiaojuan Zhang, *Icarus* **282**, 40 (2017).
- Zhencheng Tang, Jianjun Liu, Xing Wang, Xin Ren, Wangli Chen, Wei Yan, Xiaoxia Zhang, Xu Tan, Xingguo Zeng, Dawei Liu, Hongbo Zhang, Weibin Wen, Wei Zuo, Yan Su, Jianfeng Yang, Chunlai Li, *Geophysical Research Letters* **47**(22), e2020GL089499 (2020).
- G.H. Heiken, D.T. Vaniman, B.M. French, *Lunar Sourcebook, A User's Guide to the Moon* (Cambridge University Press, Cambridge, UK, 1991).
- V. Gromov, *Earth, Moon, and Planets* **80**(1), 51 (1998).
- E. Slyuta, *Solar System Research* **48**, 330 (2014).
- John Connolly, W. David Carrier, in *Proceedings of the 2023 IEEE Aerospace Conference*, NASA Document ID: 20220014634.
- H. Seifamiri, *Geotechnical properties of lunar soil* (2024).
- Preliminary Analysis of LUNA 9* (1996). <https://nsarchive2.gwu.edu/NSAEBB/NSAEBB479/docs/EBB-Moon07.pdf>.
- W.N Hess, A. J. Calio, *Apollo 11 Preliminary Science Report, SP-214* (1969). <https://www.nasa.gov/history/alsj/a11/a11psr.html>.
- W. K. Stephenson, *Apollo 12 Preliminary Science Report, SP-235* (1970). <https://www.nasa.gov/history/alsj/a12/a12psr.html>.
- F.J. Herbert, W. K. Stephenson, *Apollo 14 Preliminary Science Report, SP-272* (1971). <https://www.nasa.gov/history/alsj/a14/a14psr.html>.
- A. J. Calio, *Apollo 15 Preliminary Science Report, SP-289* (1971). <https://www.nasa.gov/history/alsj/a15/a15psr.html>.
- N.W. Hinnens, *Apollo 16 Preliminary Science Report, SP-315* (1972). <https://www.nasa.gov/history/alsj/a16/a16psr.html>.
- N.W. Hinnens, *Apollo 17 Preliminary Science Report, SP-330* (1973). <https://www.nasa.gov/history/alsj/a17/a17psr.html>.
- I. I. Cherkasov, V. V. Shvarev, *Soil Mechanics and Foundation Engineering* **10**(4), 252 (1973).
- Zhencheng Tang, Jianjun Liu, Xing Wang, Xin Ren, Wangli Chen, Wei Yan, Xiaoxia Zhang, Xu Tan, Xingguo Zeng, Dawei Liu, Hongbo Zhang, Weibin Wen, Wei Zuo, Yan Su, Jianfeng Yang, Chunlai Li, *Geophysical Research Letters* **47**(22), e2020GL089499 (2020). <https://agupubs.onlinelibrary.wiley.com/doi/pdf/10.1029/2020GL089499>.
- Jaffe, Shoemaker, *Surveyor I mission report. Part II - Scientific data and results* (1966), NTRS Document ID: 19670000738 NTRS Research Center: Legacy CDMS (CDMS). <https://ntrs.nasa.gov/citations/19670000738>.
- Haglund, *Surveyor III mission report. Part I - Mission description and performance* (1967), NTRS Document ID: 19670028267 NTRS Research Center: Legacy CDMS (CDMS). <https://ntrs.nasa.gov/citations/19670028267>.
- Jaffe, Steinbacher, *Surveyor V Mission Report. Part II - Science Results* (1967), NTRS Document ID: 19680003577 NTRS Research Center: Jet Propulsion Laboratory (JPL). <https://ntrs.nasa.gov/citations/19680003577>.
- Jaffe, Batterson, Brown, *Surveyor 6 mission report. Part 2 - Science results* (1968), NTRS Document ID: 19680011500 NTRS Research Center: Legacy CDMS (CDMS). <https://ntrs.nasa.gov/citations/19680011500>.
- V. T. Bickel, C. I. Honniball, S. N. Martinez, A. Rogaski, H. M. Sargeant, S. K. Bell, E. C. Czaplinski, B. E. Farrant, E. M. Harrington, G. D. Tolometti, D. A. Kring, *Journal of Geophysical Research: Planets* **124**(5), 1296 (2019). <https://agupubs.onlinelibrary.wiley.com/doi/pdf/10.1029/2018JE005876>.
- V. T. Bickel, D. A. Kring, *Icarus* **348**, 113850 (2020).
- Syou Maki, Han Jing, Shigeru Aoki, Mio Okuno, Yoshifumi Tanimoto, Chikako Udagawa, Shotaro Morimoto, Masao Fujiwara, Yoshihisa Fujiwara, Katsuya Inoue, (2014).
- Khalid A. Alshibli, Alsidqi Hasan, *Journal of Geotechnical and Geoenvironmental Engineering* **135**(5), 673 (2009), Publisher: American Society of Civil Engineers.
- S. Anbazhagan, I. Venugopal, S. Arivazhagan, M. Chinnamuthu, C. R. Paramasivam, G. Nagesh, S. A. Kannan, Shamarao, V. Chandra Babu,

M. Annadurai, Kasinathan Muthukkumaran, V. J. Rajesh, *Icarus* **366**, 114511 (2021).

32. Wares Chancharoen, Siwarote Siriluck, Saran Seehanam, (2021).

33. V. S. Engelschiøn, S. R. Eriksson, A. Cowley, M. Fateri, A. Meurisse, U. Kueppers, M. Sperl, *Scientific Reports* **10**(1), 5473 (2020).

34. Léonie Gasteiner, Alyona Glazyrina, Naomi Murdoch, Olfa D'Angelo, IAC-25-A3-IP-151-97770.

35. He Chunmei, Zeng Xiangwu, Wilkinson Allen, *Journal of Aerospace Engineering* **26**(3), 528 (2013), Publisher: American Society of Civil Engineers.

36. X. X. He, L. Xiao, J. Huang, *Lunar Regolith Simulant CUG-IA* (2010).

37. Yuan Zou, Huanyu Wu, Shupeng Chai, Wei Yang, Renhao Ruan, Qi Zhao, *International Journal of Mining Science and Technology* **34**(9), 1317 (2024).

38. Yongchun Zheng, Shijie Wang, Ziyuan Ouyang, Yongliao Zou, Jianzhong Liu, Chunlai Li, Xiongyao Li, Junming Feng, *Advances in Space Research* **43**(3), 448 (2009).

39. Kexin Yin, Zhichao Cheng, Jiangxin Liu, An Chen, *Planetary and Space Science* **226**, 105630 (2023).

40. Yue Teng, Shun Wang, Yifei Cui, Yong Pang, *Acta Geotechnica* **20**(5), 2327 (2025).

41. Hong Tang, Xiongyao Li, Sensen Zhang, Shijie Wang, Jianzhong Liu, Shijie Li, Yang Li, Yanxue Wu, *Advances in Space Research* **59**(4), 1156 (2017).

42. D.B. Stoeser, D.L. Rickman, S. Wilson, *Preliminary Geological Findings on the BP-1 Simulant*. <https://ntrs.nasa.gov/api/citations/20100036344/downloads/20100036344.pdf>.

43. Byung-Hyun Ryu, Cheng-Can Wang, Ilhan Chang, *Journal of Aerospace Engineering* **31**, 04017083 (2018).

44. Renhao Ruan, Wei Yang, Di Zhang, Heng-Ci Tian, Qi Zhao, Yuan Zou, Bin Yu, *Acta Astronautica* **224**, 148 (2024).

45. NASA Ames Research and Exploration Services (ARES), *OB-1 Lunar Highlands Regolith Simulant*. <https://ares.jsc.nasa.gov/projects/simulants/ob-1.html>.

46. ARES | *Exploration Science Projects | Lunar Regolith Simulants | JSC-1/IA*. <https://ares.jsc.nasa.gov/projects/simulants/jsc-1-1a.html>.

47. Yongquan Li, Jianzhong Liu, Zongyu Yue, *Journal of Aerospace Engineering - J AEROSP ENG* **22** (2009).

48. R. Allen Wilkinson, in *AIP Conference Proceedings*, pp. 1216–1223. <https://pubs.aip.org/aip/acp/article/746/1/1216-1223/605665>.

49. N. Murdoch, B. Rozitis, K. Nordstrom, S. F. Green, P. Michel, T.-L. de Lophem, W. Losert, *Phys. Rev. Lett.* **110**, 018307 (2013).

50. P. Chaikin, N. Clark, S. Nagel, in *Proceedings of a NASA Glenn Research Center virtual meeting at 2020 American Physical Society (APS) March Meeting*. <https://ntrs.nasa.gov/api/citations/20205010493/downloads/CP-20205010493%20Final.pdf>.

51. O. D'Angelo, A. Horb, A. Cowley, M. Sperl, W. T. Kranz, *npj Microgravity* **8**(1), 48 (2022).

52. P. Sánchez, K. E. Daniels, H. Jaeger, T. Shinbrot, Preprint (2023).

53. I. P. Madden, S. Muruganandam, A. Missaoui, O. Gries, J. Kollmer, O. D'Angelo, S. Sinha-Ray, *npj Microgravity* **11**(96) (2025).

54. Oliver Gaida, Olfa D'Angelo, Jonathan E. Kollmer, *Predicting granular flow – or clogging – in low gravity* (2025).

55. O. D'Angelo, Q. Yu, T. Pöschel, *Journal of Rheology* , [in print] (2026).

56. Jaffe, Alley, *Surveyor 7 Mission Report. Part 2 - Science Results* (1968), NTRS Document ID: 19680028774 NTRS Research Center: Legacy CDMS (CDMS). <https://ntrs.nasa.gov/citations/19680028774>.

57. E. N. Slyuta, *Solar System Research* **48**(5), 330 (2014).

58. Zehua Dong, Guangyou Fang, Yicai Ji, Yunze Gao, Chao Wu, Xiaojuan Zhang, *Icarus* **282**, 40 (2017).

59. Joseph F. Labuz, Arno Zang, *Rock Mechanics and Rock Engineering* **45**(6), 975 (2012).

60. B. I. Druzhininskaya, V. V. Markachev, A. V. Semenov, Yu. A. Surkov, I. I. Cherkasov, *Doklady Akademii Nauk SSSR* [Proceedings of the USSR Academy of Sciences] **199**(6), 1274 (1971), in Russian.

61. Wright Ernie, Petro Noah, *NASA SVS | CGI Moon Kit* (2019). https://svs.gsfc.nasa.gov/4720/#section_credits.

62. David Vaniman, John Dietrich, G. Jeffrey Taylor, Grant Heiken in *Lunar Sourcebook*, Grant H. Heiken, David T. Vaniman, Bevan M. French (Ed. by) (Cambridge University Press, Cambridge, United Kingdom, 1991), (1991), chapter 2, pp. 5–26.

63. David Trang, Tyra Tonkham, Justin Filiberto, Shuai Li, Myriam Lemelin, Catherine M. Elder, *Icarus* **375**, 114837 (2022).

64. F.J. Herbert, W. K. Stephenson, *Apollo 14 Preliminary Science Report*, SP-272 (1971). <https://www.nasa.gov/history/alsj/a14/a14psr.html>.

65. A. J. Calio, *Apollo 15 Preliminary Science Report*, SP-289 (1971). <https://www.nasa.gov/history/alsj/a15/a15psr.html>.

66. N.W. Hinnis, *Apollo 16 Preliminary Science Report*, SP-315 (1972). <https://www.nasa.gov/history/alsj/a16/a16psr.html>.

67. N.W. Hinnis, *Apollo 17 Preliminary Science Report*, SP-330 (1973). <https://www.nasa.gov/history/alsj/a17/a17psr.html>.

68. V. T. Bickel, C. I. Honniball, S. N. Martinez, A. Rogaski, H. M. Sargeant, S. K. Bell, E. C. Czaplinski, B. E. Farrant, E. M. Harrington, G. D. Tolometti, D. A. Kring, *Journal of Geophysical Research: Planets* **124**(5), 1296 (2019).

69. James A. McDivitt, Mission Evaluation Team, *Apollo 15 Mission Report*, SP-289 (1971). <https://www.nasa.gov/wp-content/uploads/static/history/alsj/a15/ap15mr.pdf>.